

A relation between the non-stoichiometry and hydroxyl radical generated at photocatalytic TiO₂ on 4CP decomposition

Kwang-Wook Kim^{a,*}, Eil-Hee Lee^a, Young-Jun Kim^b, Mi-Hye Lee^c,
Kwang-Ho Kim^d, Dong-Woo Shin^e

^a Korea Atomic Energy Research Institute, 150 Dukjin, Yusong, Taejeon 305-600, South Korea

^b Department of Chemical Engineering, Hannam University, Taejeon 306-798, South Korea

^c Pusan Technology Appraisal Center, Korea Technology Credit Guarantee Fund, South, 600-014, South Korea

^d Department of Inorganic Material Engineering, Pusan National University, Pusan 609-735, South Korea

^e NANO Co. Ltd., Chinju 660-882, South Korea

Received 13 December 2002; received in revised form 12 February 2003; accepted 15 March 2003

Abstract

In order to know an interrelationship between OH radical generated on the TiO₂ surface under an UV irradiation and the existence of non-stoichiometric titanium oxide of TiO_x ($0 < x < 2$) in the TiO₂, SIMS measurements and peak analyses of XPS on three kinds of TiO₂ samples were carried out, and ESR spectra of DMPO-OH adduct through spin-trapping of OH radical generated on the TiO₂ samples were measured. The generation of OH radical was approximately linear to the degree of non-stoichiometry of the TiO₂. Removal of TOC of 4CP was affected by the total surface area of the particles in the TiO₂ slurry and the non-stoichiometry within TiO₂. The particle size in the slurry depended on the mixing condition of the preparation of the slurry and the morphology of agglomeration of TiO₂ particles. The TiO₂ particles in the slurry were dispersed in much smaller size than those of TiO₂ samples on SEM.

© 2003 Elsevier Science B.V. All rights reserved.

Keywords: Photocatalytic; TiO₂; Non-stoichiometry; OH radical

1. Introduction

TiO₂ photocatalyst has attracted a great deal of attention in environmental waste-water treatment in the past decade, because it generates highly oxidative hydroxyl free radicals (OH•) which can degrade refractory organics under UV irradiation, and because it has chemical stability, non-toxicity, and is low cost [1–10]. Several kinds of photocatalytic TiO₂ including P-25 produced by Degussa are commercially available with different results in their application. The different production methods of TiO₂ bring out the changes of crystal structure, chemical composition, surface and agglomerated morphologies, physiochemical property, crystal defect structure affecting the chemical stoichiometry, etc. Such changes finally result in the difference in the destructive property of residual organics in a solution by using the TiO₂. Factors affecting TiO₂ photocatalytic reaction in a solution are amount of TiO₂ to be used, pH, dissolved oxygen, coexisting element, presence of supplemental oxidizable substance, target

organic material, and so on. A lot of research results on them have been reported [8–10]. However, it is considered that it is difficult to evaluate the intrinsic structure property of TiO₂ from those results. Therefore, some direct estimation of material properties of TiO₂ itself is necessary to understand more correctly the organic destruction.

The organic decomposition by photocatalyst is well known to be due to oxidation function of the OH free radicals made by hydroxyl groups adsorbed on TiO₂ surfaces and holes (and partly electron) induced from the photocatalytic reaction [10–16]. Accordingly, OH radicals as much as possible are required to be generated at the TiO₂ surface in order to increase the reactivity of TiO₂ for the organic decomposition. Defective surface structures of TiO₂ due to oxygen vacancy are known to affect the adsorption of water onto the TiO₂ surface and its dissociation rate into hydroxyl groups as well [12,13,16]. The defective TiO₂ means that the TiO₂ is in chemical non-stoichiometry where the ratio of Ti to O within TiO₂ is less than 2. Therefore, a measurement of degree of non-stoichiometry of TiO₂ is considered to give more important information to help understand the intrinsic property of TiO₂. However, there are few papers

* Corresponding author. Tel.: +82-42-868-2044; fax: +82-42-868-2042.
E-mail address: nkwkim@kaeri.re.kr (K.-W. Kim).

about the effect of the non-stoichiometry of TiO_2 on the amount of the generated OH radicals.

In this work, quantitative and qualitative comparisons of the chemical non-stoichiometries of three kinds of TiO_2 samples were studied by XPS, SIMS analyses and a relative comparison of the amount of OH radicals generated from TiO_2 under UV irradiation was carried out by using a ESR spectrometer, and then with those results, it was tried to find how the existence of non-stoichiometry within TiO_2 affects the generation of OH radical which can oxidize organics in solution, not to find the absolute superiority of a TiO_2 sample among the tested samples as a photocatalyst.

2. Experimental

Three kinds of TiO_2 P-25 of Degussa, NT-20 and NT-C of NANO Co. Ltd. were used in this work as received. Demineralized water of $18.2 \text{ M}\Omega$ prepared by distilling twice and an ion-exchanger (Mill-Q plus) was used for the preparation of TiO_2 slurry. A 450 W mercury vapor UV lamp (Hanovia Co.) was used for the photocatalytic reaction, and a Vycor adsorption sleeve to cut off the wave lengths less than 250 nm was placed between the lamp and a quartz immersion well (Ace Glass Co.) inside which the lamp was put. The quartz immersion well kept at $25 \pm 0.5^\circ\text{C}$ by circulating coolant from a chiller was inserted into a Pyrex tube reactor (Ace reaction vessel 7863) of 500 ml. An amount of 1.5 g/l TiO_2 slurry of 1000 ml was circulated inside the reactor through a pump and an external reservoir. A magnetic bar was placed at the bottom of the reactor in order to disperse homogeneously the TiO_2 particles within the reactor without sedimentation during the photocatalytic reaction. TiO_2 slurry was prepared by mixing thoroughly TiO_2 powders in water with magnetic stirring and sonification, and then put into the photoreactor.

For the organic destruction test, the TiO_2 slurry containing dissolved 4CP (4-chlorophenol) of 50 ppm was sampled at regular intervals and then its total organic carbon was measured with a TOC analyzer (Shimadzu TOC-5000A). Relative amounts of OH radicals generated at the TiO_2 sample surfaces were evaluated by an electron spin resonance (ESR) technique. The OH radical generated at the TiO_2 surface under UV irradiation is very short-lived and very reactive, so a spin-trapping agent of 5,5'-dimethyl-1-pyrroline-*N*-oxide (DMPO), which converts a short-lived free radical into a relatively long-lived free radical product, was used to make the OH radical form more stable spin adduct with DMPO in the solution [17–19]. The OH radical spin adduct of DMPO was prepared through sampling the TiO_2 slurry under UV irradiation instantaneously with a syringe containing a constant volume of 20 mM DMPO. The solution was quenched with dry ice, and then the ESR signal of the solution was measured by an ESR spectrometer (Bruker EMX 10/12).

TiO_2 particle sizes dispersed in slurry were measured by a particle size analyzer (Microtrac UPA-150) and the bulk densities of TiO_2 samples were measured by a pycrometer (Micrometrics AccuPyc 1330). In order to evaluate the non-stoichiometry of TiO_2 , secondary ion mass spectrometry (SIMS, Cameca-ims 4f) using an O_2^+ ion beam and X-ray photoelectron spectroscopy (XPS, VG scientific ESCALB-200R) peak deconvolution technique were used. Also, electron probe microanalyzer (EPMA, JEOL JXA 8600 with EDX detector) was used for the measurement of composition of compounds within TiO_2 .

3. Results and discussion

Fig. 1 shows XRD patterns showing the crystalline structures of the TiO_2 samples. As P-25 of Degussa has been

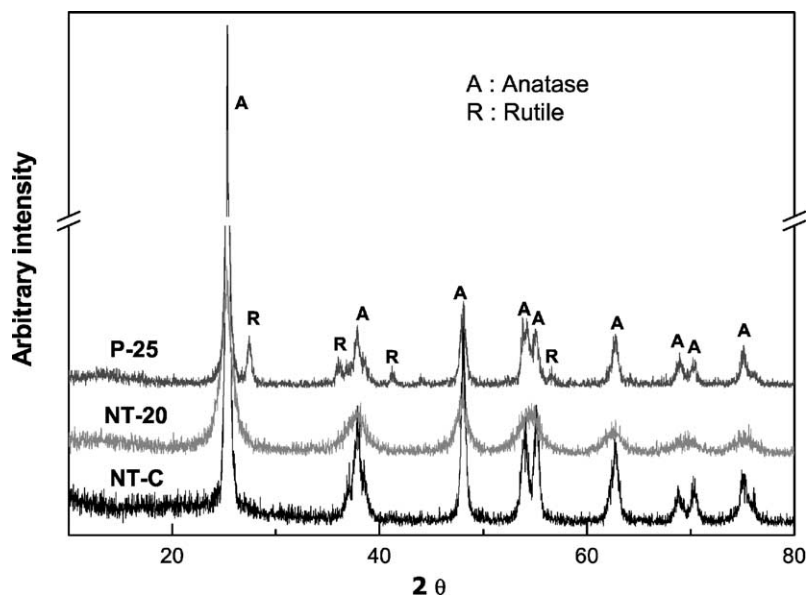


Fig. 1. XRD patterns of TiO_2 samples.

Table 1
Major elements and their relative atomic mol% of TiO₂ samples

| Sample | Ti | Fe | S | Si |
|--------|-------|------|------|------|
| P-25 | 99.4 | – | – | 0.6 |
| NT-C | 99.39 | – | 0.42 | 0.19 |
| NT-20 | 97.98 | 0.48 | 0.82 | 0.55 |

known to have a composite structure of anatase and rutile [20], the sample shows peaks at 25.3, 48.1, and 55.1° for an anatase structure and 27.4, 36.1, and 54.3° for a rutile structure. On the other hand, NT-C and NT-20 samples of NANO Co. Ltd. have only peaks for an anatase structure without a rutile one. Major components within bulks of the TiO₂ samples analyzed by EPMA are shown in Table 1. P-25 consists of almost Ti with a little portion of Si of about 0.6%. However, NT-C contains S of 0.4% together with Si of about 0.2%. NT-20 contains Fe of about 0.5%, S of 0.8%, and Si of 0.5%.

Fig. 2 shows SIMS results showing the secondary ion beams coming from collision of primary beam of O₂⁺ against the TiO₂ sample surfaces. Several kinds of cluster ions from the recombination of ions brought out by the primary ion beam were observed. The intensities of Ti⁺ ion for P-25, NT-20, and NT-C are almost the same, but amounts of titanium oxide cluster ions such as TiO⁺, TiO₂⁺, Ti₂O⁺, and Ti₂O₂⁺, etc. are in the order of NT-C > NT-20 > P-25. The result can be explained to be because more non-stoichiometric Ti oxide structure of TiO_x (0 < x < 2) exists at the surface of NT-C than at the surfaces of NT-20 and P-25, so more various titanium oxide cluster ions are emitted from the NT-C sample by the primary ion beam.

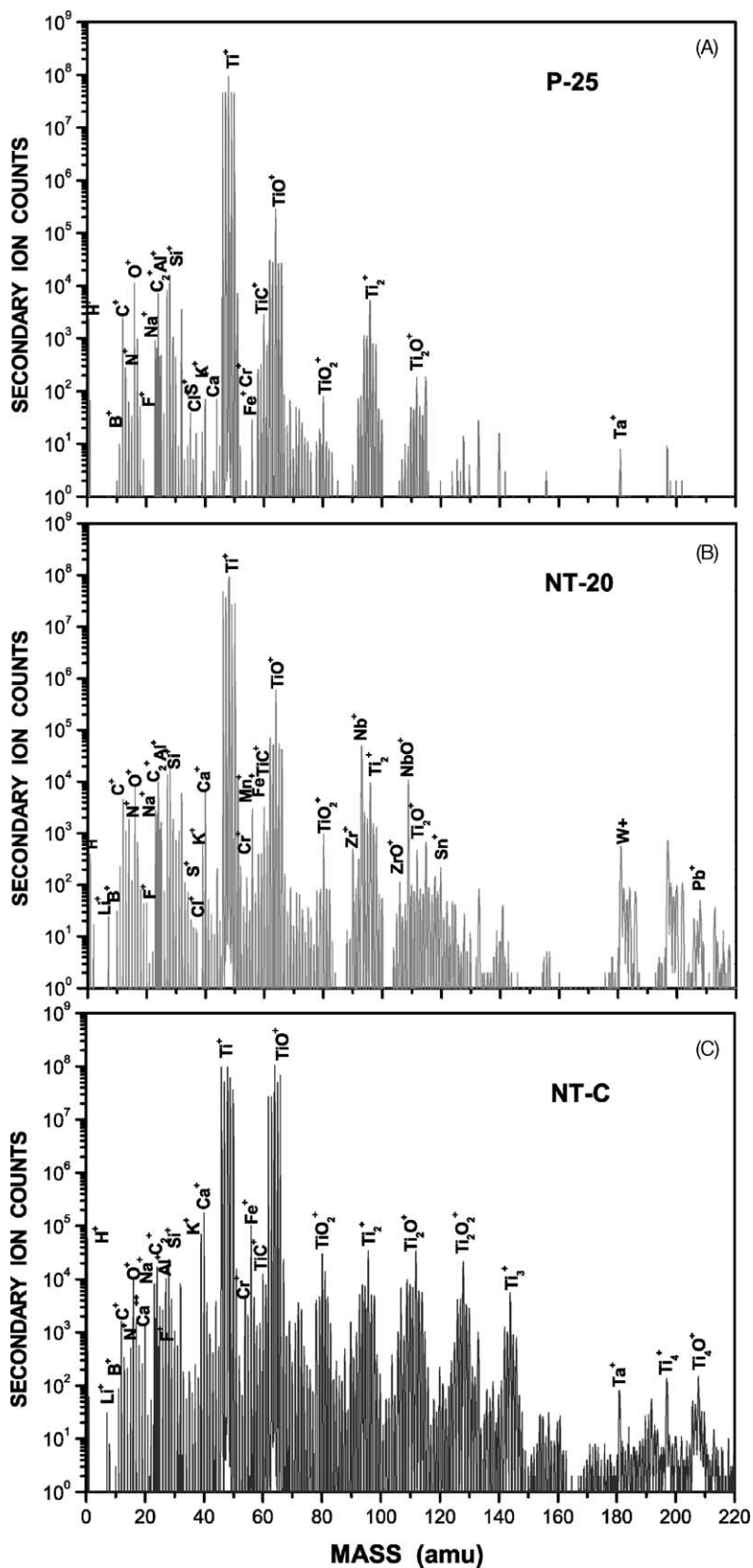
XPS spectra of species of O 1s and Ti 2p_{3/2} of the TiO₂ samples and their peak deconvolution results are shown in Fig. 3 to estimate the statuses of TiO₂ sample structures. If TiO₂ is perfect in stoichiometry, the Ti 2p_{3/2} peak should be fitted with only TiO₂ species of a binding energy of 458.8 eV. However, the curve-fitting of Ti 2p_{3/2} using only TiO₂ species did not give a satisfying result. There were some deviations around in the range of 456–457 eV. According

to the XPS database showing binding energies of titanium compounds [21], the binding energies for TiO_{1.5}, TiO, and Ti are 456.1, 455.1, and 454 eV, respectively. The less number of oxygen atoms combined to Ti in the species is, the smaller the binding energy of the species is. Therefore, in the case of NT-C, for instance, the Ti 2p_{3/2} peak could be best deconvoluted with allotting another species at 457.8 eV less than 458.8 eV of TiO₂ species. The newly added species is considered to be Ti^{δ+} (0 < δ < 4) namely, TiO_x (0 < x < 2) of non-stoichiometric oxide. In order to check soundness of the deconvolution results of Ti 2p_{3/2} peaks in Fig. 3, the deconvolution result of O 1s peak of TiO₂ sample should be taken into consideration together with the Ti 2p_{3/2} peak. If the sample is only TiO₂, the O 1s peak should be fitted with the binding energy of 529.9 eV for TiO₂ in the same way as the Ti 2p_{3/2} peak case. However, the O 1s peak was not represented with only TiO₂ species as well. The binding energy of Si oxide detected at NT-C (see Table 1) of SiO₂ for O 1s is about 530.7 eV. Tiny amounts of impurities such as Ta, Al, Fe, etc. which were experimentally detected at the samples by XPS and were shown in Fig. 2, exist in the TiO₂ samples. The binding energies of such impurity metal oxides for O 1s range approximately from 530 to 531 eV. The binding energy of Ti oxide such as TiO_x for O 1s is reported to be about 530.7 for O 1s [22]. However, the O 1s peak could not completely be deconvoluted with both of a peak for the TiO₂ species around 529.9 eV and a peak for the species of TiO_x and the metal oxides including SiO₂ around 530–531 eV. An additional peak around 532 eV was necessary. The species for the additional peak is considered to be some species with C–O bonds [22]. In order to confirm it, C 1s peak is shown in Fig. 4. There is some peak around 288–289 eV beside the peak for carbon at 284.5 eV. Many kinds of C–O species for C 1s are reported to be located around 288.5–289 eV [22]. From this result, it is understood that some C–O compounds exist on the TiO₂ sample surface. Therefore the O 1s peak is concluded to have C–O bonded species at 530–531 eV. The O 1s peaks of TiO₂ samples could be the best deconvoluted with the species of TiO₂, TiO_x + MO₂, and C–O compounds. Table 2 shows areas and binding energies of the deconvoluted peaks of Ti

Table 2
Areas and binding energies of deconvoluted peaks of Ti 2p_{3/2} and O 1s peaks of XPS of TiO₂ samples, and calculated TiO_x/TiO₂ and relative atomic mole ratios of TiO₂^a

| Sample | | Ti 2p _{3/2} | | O 1s | | | T2/T1 | O/Ti atomic ratio of TiO ₂ |
|--------|------|------------------------|------------------------|------------------------|------------------------|------------|-------|---------------------------------------|
| | | T1 (TiO ₂) | T2 (TiO _x) | O1 (TiO ₂) | O2 (TiO _x) | O3 (Other) | | |
| P-25 | BE | 458.6 | 456.8 | 529.8 | 530.6 | 532.2 | 0.338 | 2.094 |
| | Area | 6342.5 | 2144.4 | 4869.2 | 5466.6 | 5684.9 | | |
| NT-20 | BE | 458.6 | 457.6 | 529.5 | 530.3 | 531.9 | 0.469 | 2.192 |
| | Area | 8711.4 | 4087.0 | 7001.3 | 9931.4 | 4571.3 | | |
| NT-C | BE | 458.6 | 457.8 | 529.1 | 529.9 | 531.0 | 0.681 | 2.132 |
| | Area | 12534.1 | 8530.4 | 9800.1 | 13666.6 | 3266.3 | | |

^a BE: binding energy (eV) for deconvolution; TiO₂ atomic ratio: (O1/O sensitivity factor of 0.66)/(T1/Ti sensitivity factor of 1.8).

Fig. 2. Mass spectra of TiO_2 samples by SIMS.

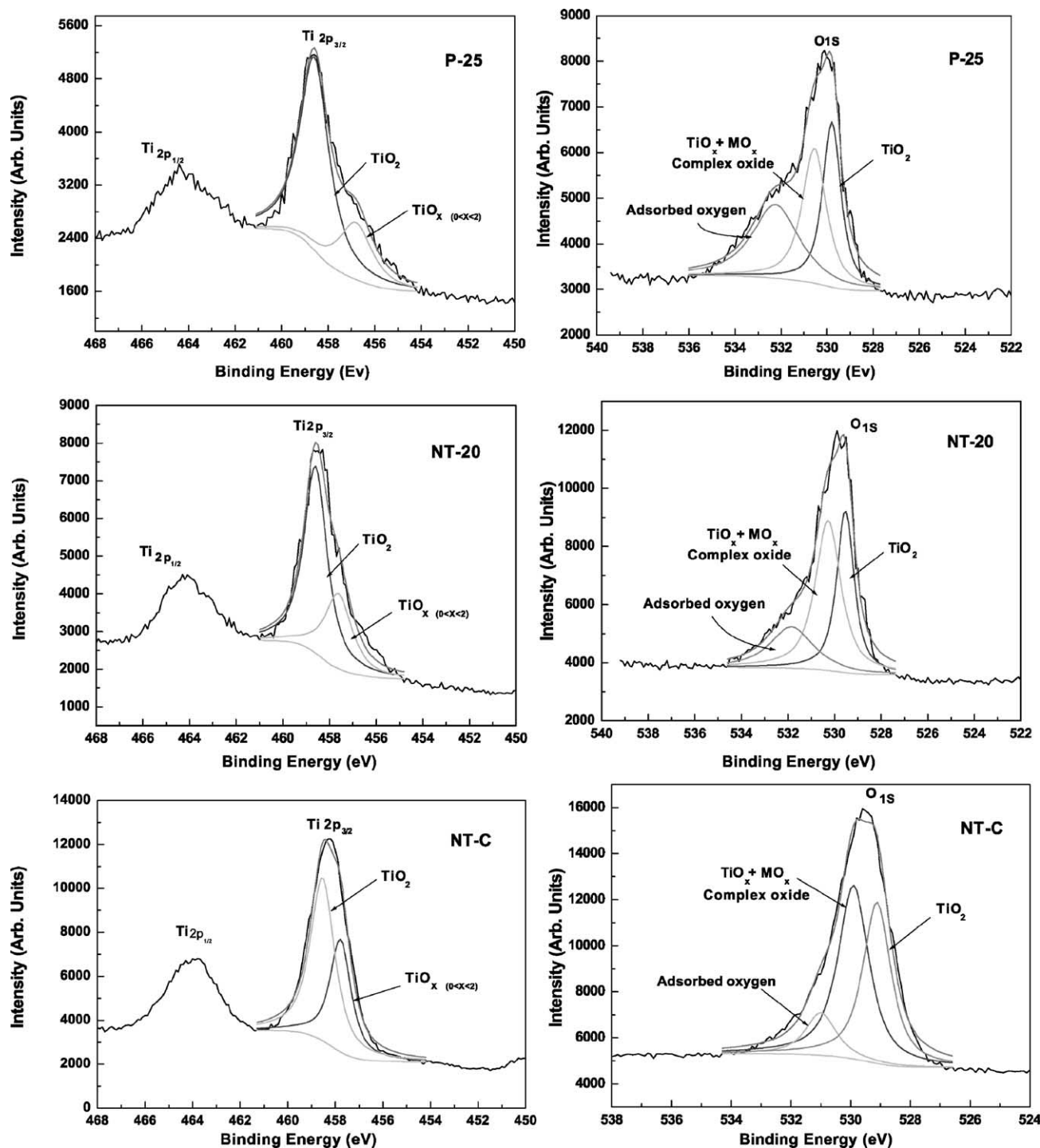


Fig. 3. Deconvoluted XPS peaks of Ti 2p_{3/2} and O 1s of TiO₂ samples.

2p_{3/2} and O 1s peaks for the TiO₂ samples, and it also shows ratios of TiO_x/TiO₂ calculated from the area, which means the degree of non-stoichiometry. And the deconvoluted areas of Ti 2p_{3/2} for TiO₂ and O 1s for TiO₂ are normalized with atomic sensitivity factors. The sensitivity factors for Ti 2p_{3/2} and O 1s peaks are 0.66 and 1.8. The ratios of the normalized areas are the atomic ratios of Ti and O of the

TiO₂ components of the samples, and are shown in Table 2 as well. All the ratios are almost 2. It means that the peak deconvolutions carried out in Fig. 3 to evaluate the degree of non-stoichiometry within the samples were reasonable and sound. The order of the degree of non-stoichiometry for the samples is NT-C > NT-20 > P-25 like the result by SIMS, as shown in Table 2. The TiO_x/TiO₂ ratios are

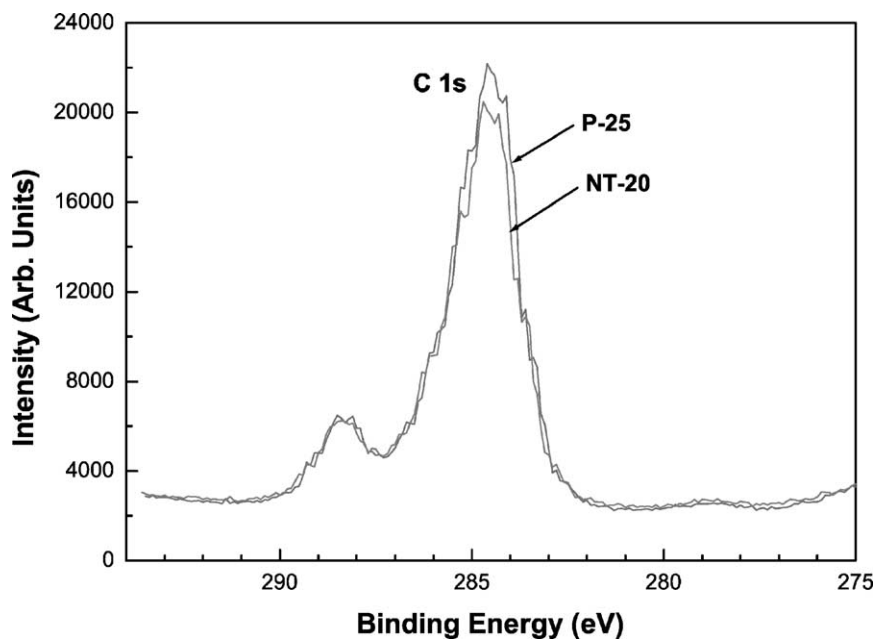


Fig. 4. Narrow scanned XPS peak of C 1s of P-25 and NT-20 samples.

30–70%, which are higher than expected. The reason is considered to be because XPS shows property only within a few Å from the surface and because the surface structure of oxide is unstable unlike the bulk structure of oxide. Therefore the measured $\text{TiO}_x/\text{TiO}_2$ ratio does not represent the average value within the sample bulk, but that near the surface. So the ratio is considered to appear high.

The defected structure due to oxygen vacancy on TiO_2 affects adsorption of water on its surface and the dissoci-

ation rate of the water into hydroxyl groups and protons [12,13,16,22]. A TiO_2 with more portion of TiO_x resulting from the defected structure can have more OH group on its surface, so such TiO_2 is considered to be able to generate more OH radicals at the surface under UV irradiation. The catalytic oxide electrodes such as RuO_2 and IrO_2 , which can generate OH radicals on its surface during electrolysis, have been known to have some portion of non-stoichiometric structure in their surface to generate OH radical through the

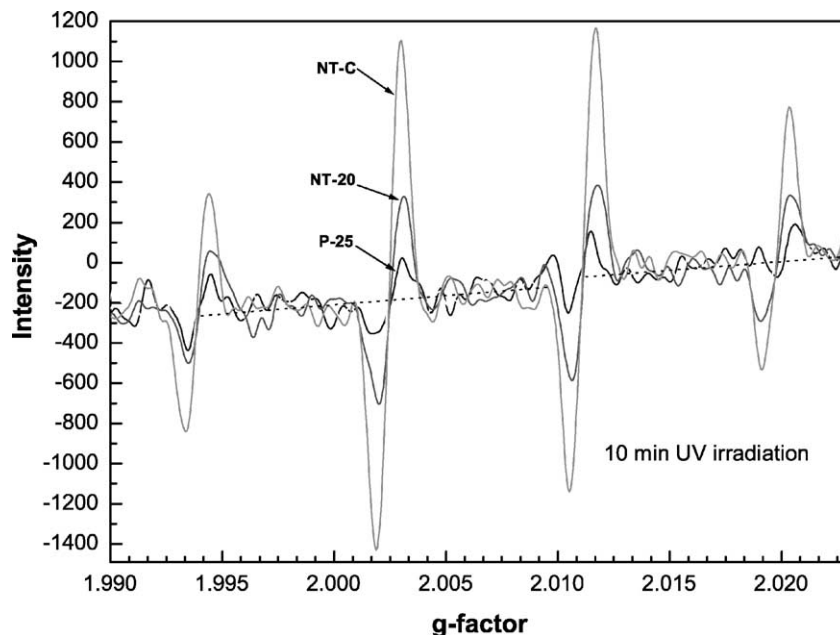


Fig. 5. ESR spectra of DMPO-OH radical adduct after UV-irradiation of TiO_2 samples.

adsorption of hydroxyl groups from water similarly to the TiO_2 catalyst case [23–27]. In this work, amounts of OH radicals generated on the TiO_2 sample surfaces were identified. The existence of unstable and very short-lived OH radical in solution can be indirectly detected through the measurement of an OH radical spin adduct of DMPO by an ESR spectrometer [17–19]. A certain volume of TiO_2 slurry without 4CP was instantly taken out of the reactor under UV irradiation with a syringe containing DMPO already, and then their ESRs were measured. The results are shown in Fig. 5. The typical spectra of DMPO-OH adduct ESR with peaks of 1:2:2:1 [17,28] was observed. The relative spectrum amplitudes means the relative amounts of OH radicals generated on the TiO_2 sample surfaces. The amounts were expected to change according to the degrees of non-stoichiometries shown in Figs. 2 and 3. The order of the peak amplitudes is NT-C > NT-20 > P-25 like the results in Figs. 2 and 3. In the TiO_2 slurry, only the TiO_2 particles exposed to incident UV light are considered to be photo-excited to generate the holes and electrons, but the TiO_2 particles screened off UV source behind the TiO_2 particles exposed to UV light is not so. In that case, if it is assumed that the numbers of TiO_2 particles dispersed in the reactor are enough, the total area of TiO_2 particles exposed perpendicularly to incident UV light in the reactor is considered to be approximately the same at any moment. Most of the OH radicals generated at the TiO_2 surface in a slurry solution volume taken off the reactor by the syringe is consumed to react with DMPO in the syringe, because the slurry solution did not contain 4CP. Under the same UV source and the same total TiO_2 area irradiated by UV in the solution, the difference of measured ESR is considered to be due to the difference of TiO_2 surface property to affect the generation of OH radicals, in other word,

difference of non-stoichiometry of TiO_2 . Therefore the differences of amounts of OH radicals shown in Fig. 5 are considered to be due to the degrees of non-stoichiometries existing at the surfaces of the TiO_2 samples. From these results, the OH radical generation can be said to be affected by the non-stoichiometry existed in TiO_2 samples, even if the TiO_2 samples show the same anatase structure. Organic materials dissolved in TiO_2 slurry are known to be decomposed into water and carbon dioxide by the highly oxidative OH radicals generated on the TiO_2 surface [1–20]. Fig. 6 shows the change of TOC of 4CP in TiO_2 slurries of 1.5 g/l with time. An inset showing the removal yield of 4CP TOC in the TiO_2 slurry systems after UV irradiation of 90 min is included in Fig. 6 as well. The order of TOC removal yields by the TiO_2 samples are NT-C \approx P-25 > NT-20. Because all the TiO_2 particles in the reactor have the same possibilities to be exposed to UV light, if the particles move very fast in the reactor, the total amount of OH radicals consumed in the solution for a certain time to attack the 4CP in the reactor is considered to depend on the total surface area of all the TiO_2 particles moving in the reactor as well as the non-stoichiometry at the TiO_2 to affect the generation of the OH radicals. The reason that the TOC removal yields of P-25 and NT-C are almost the same, although the non-stoichiometry of NT-C is higher, is considered to be because the total particles areas of P-25 is higher in the reactor so that the amounts of total generated OH radicals in a unit volume are similar.

In order to confirm the fact, actual particle size distributions of TiO_2 samples in slurry were measured and are shown in Fig. 7, and their average sizes are given in Table 3. The morphologies by SEM and particle sizes of dry P-25, NT-20, and NT-C samples are shown in Fig. 8 and Table 3.

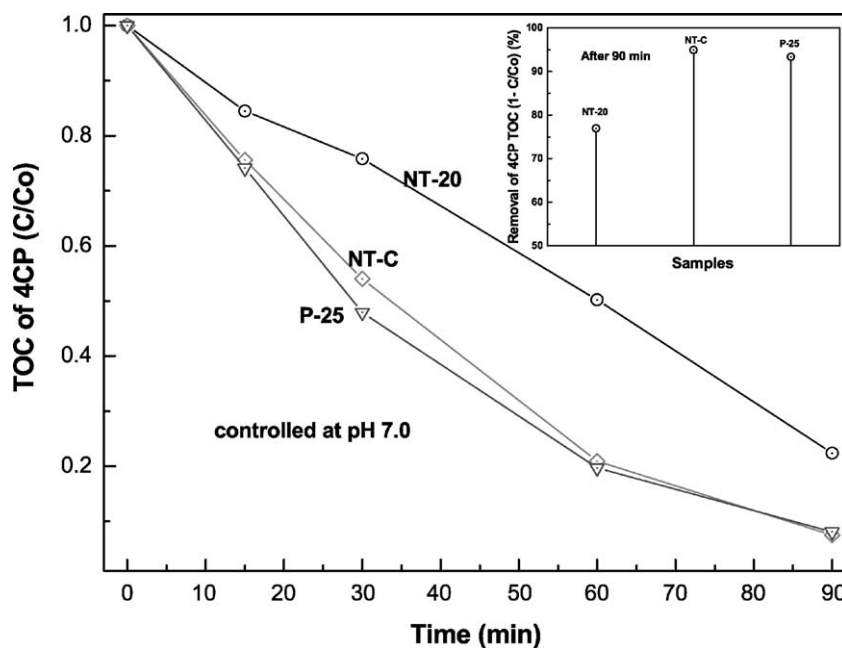


Fig. 6. Changes of TOC of 4CP in the TiO_2 slurry systems with time.

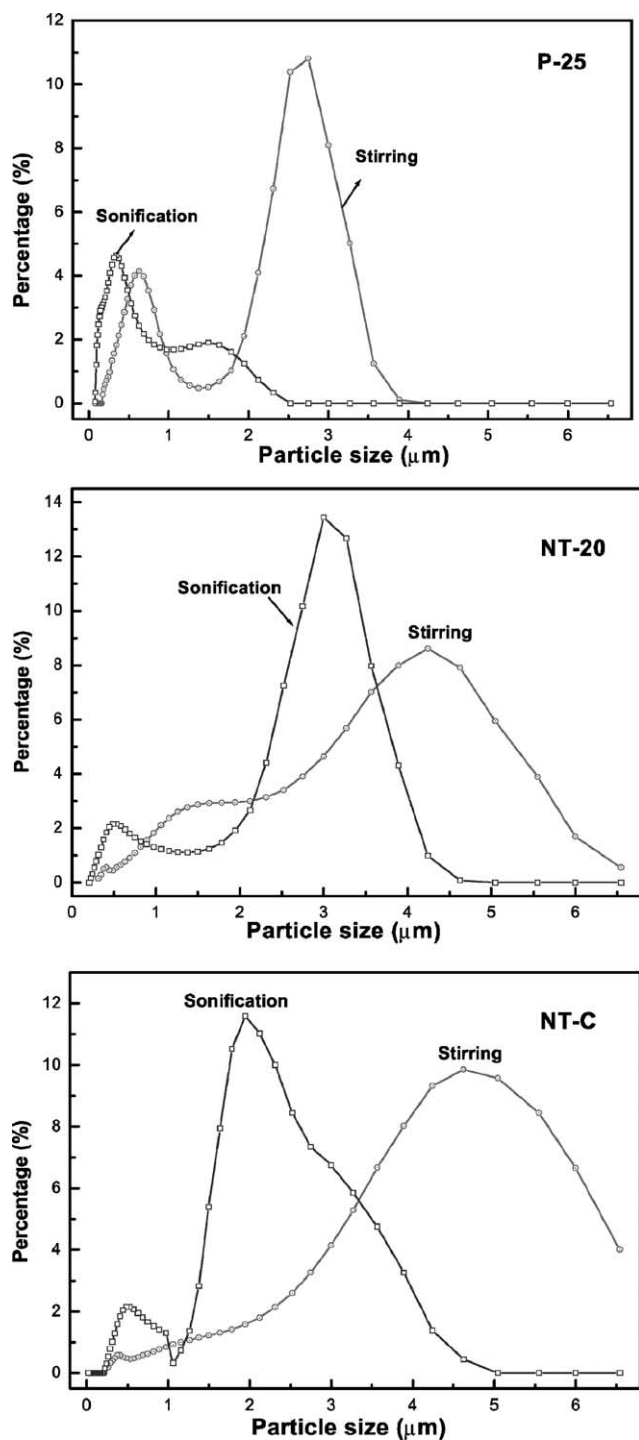


Fig. 7. Particle size distributions of TiO₂ samples with mixing condition.

The NT-20 and NT-C samples have morphologies agglomerated with distinct particles of about 0.1 μm and about 0.5 μm in diameter, respectively. However, the P-25 sample has a soft-looking morphology of clusters agglomerated with much finer particles. The average size and the particle size distribution of TiO₂ in slurry change with the mixing conditions for preparation of TiO₂ slurry, as shown in

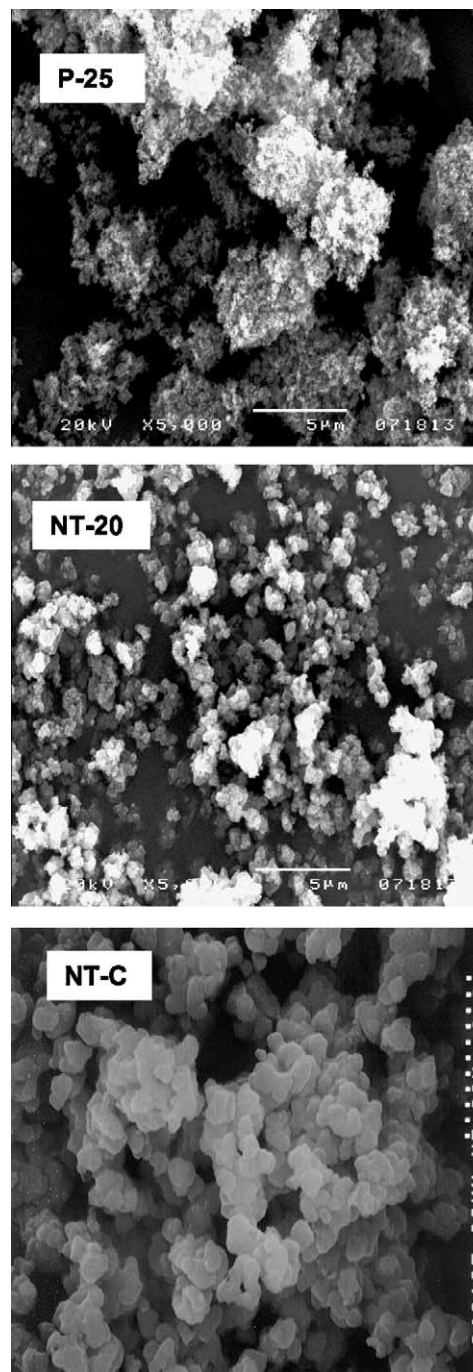



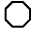



Fig. 8. SEM photographs of TiO₂ samples.

Fig. 7 and Table 3. The cluster size of P-25 on SEM is about 4–5 μm, but its average size in a solution after the slurry with magnetic stirring and sonification is reduced to about 0.34 μm which is much smaller than that of NT-C of about 2.1 μm prepared in the same condition. The reason is considered to have a relation with the status of agglomerated morphology of TiO₂ and a mixing power applied in slurry. The particle size distribution of P-25 in slurry after the magnetic stirring has a clear bimodal particle size distribution

Table 3
Average size of crystalline, dry particle, and dispersed particle in solution of TiO₂ samples^a

| | Crystalline size by TEM (nm) | Single particle | Agglomerated particle size (μm) | Mixing | Dispersed particle size in solution (μm) |
|-------|------------------------------|--|--|--------|--|
| P-25 | ~20 | 4–5  | 4–5 | M | 0.52 (46%), 2.49 (54%) |
| NT-20 | ~4–5 | ~0.1  | 2–3  | M + S | 0.34 |
| | | | | M | 2.96 |
| NT-C | ~25 | 0.4–0.6  | ~8  | M + S | 0.48 (77%), 2.96 (23%) |
| | | | | M | 3.8 |
| | | | | M + S | 2.09 |

^a M: magnetic mixing; S: sonification mixing.

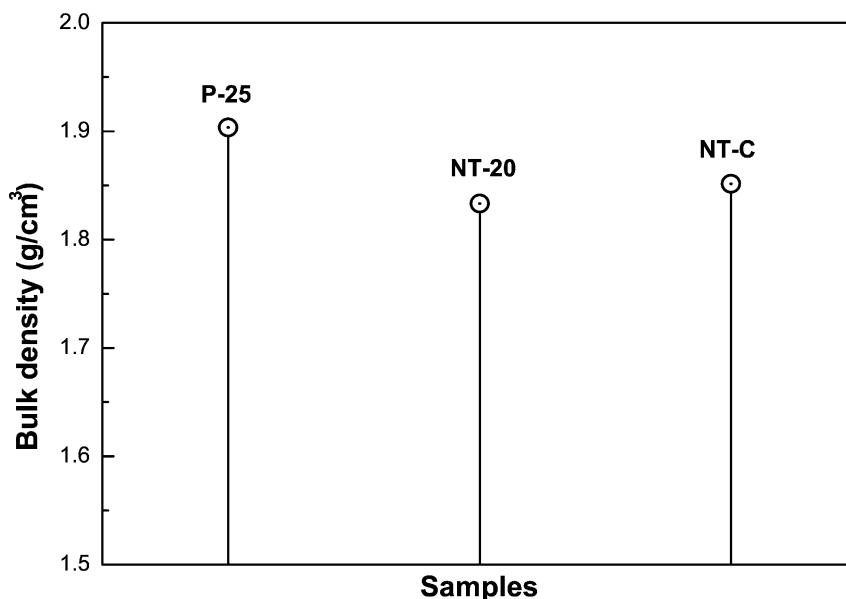


Fig. 9. Bulk densities of TiO₂ samples.

consist of two average sizes of 0.52 μm (46%) and 2.49 μm (54%). In the case of NT-20 after the magnetic stirring and sonification, the slurry also has a particle size distribution with two average sizes of 0.48 μm (77%) and 2.96 μm (23%). These results mean that a total area of all the particles in slurry should be considered by actual measurement in slurry, not by SEM of dry sample. Now that the average

particle sizes of the TiO₂ samples in slurry has been obtained, if the bulk densities of the samples are known, one can calculate relative ratios of total particle surface areas in slurry at the same TiO₂ concentration. The bulk densities of P-25, NT-20, and NT-C samples were measured and the values are shown in Fig. 9. With the bulk densities and the average particle sizes shown in Table 3, the relative ratios

Table 4
Relative ratios of total surface area of particles in the slurry, total OH radical generation, and removal yield of 4CP TOC of TiO₂ samples

| | Relative ratio of total surface area | Relative ratio of generated OH radical at TiO ₂ surface | Relative ratio of total generated OH radical within reactor | Relative ratio of 4CP destruction |
|------------------|--------------------------------------|--|---|-----------------------------------|
| $R_{P-25/P-25}$ | 1 | 1 | 1 | 1 |
| $R_{NT-20/P-25}$ | 0.3394 | 2.576 | 0.874 | 0.819 |
| $R_{NT-C/P-25}$ | 0.1672 | 6.551 | 1.095 | 1.017 |

of total particle surface areas in slurry on the basis of P-25 were evaluated, as shown in Table 4. The total area of P-25 in slurry is three times and 5.9 times higher than those of NT-20 and NT-C, respectively. As mentioned above, the relative amplitude of the OH radical spin adduct of DMPO at a g -factor in Fig. 5 means the relative OH radical generated only at the TiO₂ surface exposed to UV light due to the degree of non-stoichiometry of TiO₂. The relative amplitudes of the OH radical at a g -factor of 2.003 are shown in Fig. 4. Now the relative total area of all the particles in reactor and the relative OH radical generated only at the TiO₂ surface exposed to UV light are known. Therefore, with the assumption that all the TiO₂ particles in the reactor have the same possibilities to be exposed to UV light in the reactor because the particles move fast, the relative total amount of OH radicals generated in the reactor can be evaluated as a product of the two calculated values. As the 4CP decomposition is linear to a number of contacting times between 4CP and OH radicals in the reactor, the TOC removal yield of 4CP in the reactor in a certain time is considered to be linear to the amount of total OH radicals generated in the reactor. In Table 4, the relative total amounts of OH radicals generated in the reactor and the relative removal yields of TOC of 4CP with respects to P-25 are represented. The two values are 1.09 and 1.02 for the case of NT-C and are 0.87 and 0.82 for the case of NT-20, respectively. The two values for each case are close. That means that an amount of OH radicals generated in a photocatalytic reactor, which are used for the organic destruction, depend on the degree of non-stoichiometry within a TiO₂ sample and the total area of all the particles in the reactor at the same time.

4. Conclusion

The order of the degree of non-stoichiometry of TiO_x ($0 < x < 2$) within the TiO₂ samples of P-25, NT-C, and NT-20 estimated by SIMS measurements and peak analyses of XPS was NT-C > NT-20 > P-25. The amount of OH radicals measured by a DMPO-OH adduct ESR method was affected by the non-stoichiometric titanium oxide in the TiO₂. The 4CP decomposition depended on the non-stoichiometry of the TiO₂ samples and the total area of all the particles in slurry. The mixing condition for preparation of TiO₂ slurry had considerable affect on the particle size distribution in slurry.

Acknowledgements

This work was supported by Ministry of Commerce, Industry and Energy in South Korea.

References

- [1] A. Fujishima, K. Honda, *Nature* 238 (1971) 37.
- [2] B. Kraeutler, A.J. Bard, *J. Am. Chem. Soc.* 100 (1977) 5985.
- [3] D.F. Ollis, A.L. Pruden, *J. Catal.* 82 (1983) 404.
- [4] R.W. Matthews, *J. Chem. Soc., Faraday Trans.* 80 (1984) 457.
- [5] J. Sabate, M.A. Anderson, *J. Catal.* 27 (1991) 166.
- [6] L.P. Childs, D.F. Ollis, *J. Catal.* 67 (1981) 35.
- [7] N. Djeghri, S.T. Teichner, *J. Catal.* 62 (1980) 99.
- [8] M. Litter, *Appl. Catal. B: Environ.* 23 (1999) 89.
- [9] A. Hagfeldt, M. Gratzel, *Chem. Rev.* 95 (1995) 4.
- [10] N. Serpone, E. Pelizzetti, *Photocatalysis, Fundamentals and Applications*, Wiley, New York, 1989.
- [11] G. Lu, A.L. Linsebigler, J.T. Yates Jr., *J. Phys. Chem.* 98 (1994) 11733.
- [12] R.L. Kurtz, R. Stockbauer, T.E. Madey, *Surf. Sci.* 218 (1989) 178.
- [13] S. Bourgeois, F. Jomard, M. Perdereau, *Surf. Sci.* 278 (1992) 349.
- [14] M.B. Hugen Schmidt, L. Gamble, C.T. Campbell, *Surf. Sci.* 302 (1994) 329.
- [15] R.L. Kurtz, R. Stockbauer, T.E. Madey, E. Roman, J.L. De Segovia, *Surf. Sci.* 218 (1989) 178.
- [16] P.B. Smith, S.L. Bernasek, *Surf. Sci.* 188 (1987) 241.
- [17] S. Echigo, H. Yamada, S. Matsui, S. Kawanishi, K. Shishida, *Water. Sci. Technol.* 34 (1996) 81.
- [18] C.-S. Lai, L.H. Piette, *Biochem. Biophys. Res. Commun.* 78 (1977) 51.
- [19] K. Makino, M.M. Mossoba, P. Riesz, *J. Am. Chem. Soc.* 105 (1982) 3537.
- [20] K.-S. Jung, H.-I. Lee, *J. Korean Chem. Soc.* 41 (1997) 682.
- [21] J.F. Mouler, W.F. Stickle, P.E. Sobol, K.D. Bomben, *Handbook of X-ray Photoelectron Spectroscopy*, Physical Electronics Inc., 1995.
- [22] A.L. Linsebigler, G. Lu, J.Y. Yates, *Chem. Rev.* 95 (1995) 735.
- [23] S. Trasatti, *Electrode of Conductive Metallic Oxides, Part A*, Elsevier, Amsterdam, 1980.
- [24] D. Galizzioli, F. Tantarini, S. Trasatti, *J. Appl. Electrochem.* 5 (1975) 203.
- [25] D. Galizzioli, F. Tantarini, S. Trasatti, *J. Appl. Electrochem.* 4 (1974) 57.
- [26] R.S. Teo, J. Orehotsky, W. Visscher, S. Srinivasan, *J. Electrochem. Soc.* 128 (9) (1981) 1900.
- [27] K.-W. Kim, E.-H. Lee, J.-S. Kim, K.-H. Shin, K.-H. Kim, *Electrochim. Acta* 460 (2001) 915.
- [28] R.A. Floyd, L.M. Soong, *Biochem. Biophys. Res. Commun.* 74 (1) (1977) 79.